Experimental Thermal and Fluid Science 78 (2016) 65–74

Contents lists available at ScienceDirect

Experimental Thermal and Fluid Science

journal homepage: www.elsevier.com/locate/etfs

Dependence of the blast load penetrating into a structure on initial conditions and internal geometry

O. Ram [1], E. Nof [1], O. Sadot *

Shock Tube Laboratory, Protective Technologies R&D Center, Faculty of Engineering Sciences, Ben-Gurion University of the Negev, Beer-Sheva, Israel

ARTICLE INFO

Article history:
Received 15 February 2016
Received in revised form 13 May 2016
Accepted 14 May 2016
Available online 14 May 2016

Keywords:
Blast-structure interaction
Blast waves
Impulse effects
Exploding wire
Scaling
Risk assessment
Explosion effects

ABSTRACT

An experimental study investigated the dependence of the blast load penetrating into a structure on initial conditions and internal geometry. The imposed pressure and impulse profiles at the structures' frontal façades were varied to generate initial conditions with very different pressures but similar peak impulses to which structural models of varying complexity were exposed. Results show that the peak impulse recorded at the models' back wall, the target wall, is independent of internal geometry. However, the pressure profiles at the target wall depend heavily on internal geometry in terms of both peak overpressure and wave diffraction pattern. Moreover, the pressure profile developed inside the structure depends strongly on the imposed impulse rather than the imposed pressure profile at the frontal façade. Repeated reflections inside the structure were found to effectively filter out high-frequency pressure changes inside the structure, leading to the possibility of rapid prediction tools for more complex structures. For the first time, a strong indication was found that a scalable time constant can be attributed to a complex structure that characterizes the load developing inside. Based on these findings, an application is presented in which forming a similar impulse is sufficient for correctly simulating large explosions in scaled-down models.

1. Introduction

The start of the 21st century marked an alarming rise in global terror attacks targeting civilians. The increasing number of incidents, combined with their expanding variety and sophistication, has alerted security authorities to the need for developing tools to respond to this unexpected reality. Urban centers have been prone to various threats including car bombs, suicide attacks, improvised explosive devices (IEDs), mortars, and more. The payloads used in such circumstances can range from several hundreds of grams up to several hundreds of kilograms of T.N.T.-equivalent charge. Most civilian structures cannot withstand explosive events, nor are they designed to do so. Addressing these vulnerabilities calls for new security protocols for structural design and for sensitive buildings to be retrofitted with countermeasures. In order to integrate a variety of security concerns, structural engineers must be able to resolve complex questions. For example, in order to evaluate the load penetrating a building in the event of an external explosion, should one consider the blast pressure or the positive impulse applied on the building's frontal façade? How do various internal designs affect the developing load in a specific room? What simplifying assumptions are appropriate in facilitating prompt decision-making in the face of imminent attacks?

Currently, tools are available to answer these difficult questions; however, they require considerable resources, rendering them impractical for wide applications. This study aims to understand the fundamental physics governing load development inside structures and to highlight the dominant parameters involved. The insights realized here are useful in developing more rapid prediction tools for assessing blast survivability inside structures.

Studies regarding shock and blast wave interaction with structures can be divided into two main groups. The first group usually deals with the physical mechanisms of shock-structure interaction, development of flow fields, and material response while the second group includes studies more focused on applications to structural design, load assessment, and survivability following an explosive event.

Limiting the discussion to studies concerning the gas dynamics associated with blast and shock impingement, one finds a large body of research concerning the propagation of shock waves through sets of geometrical obstacles. These obstacles include baffles [1–4], plates [5–9], porous materials [10–14], aqueous foams [15–17], granular media [18–20], and more. These studies are generally performed in a laboratory setup in which intricate shock

* Corresponding author.
E-mail address: sorens@bgu.ac.il (O. Sadot).
[1] Equally contributed.

http://dx.doi.org/10.1016/j.expthermflusci.2016.05.012
0894-1777/

diffraction and reflections can be recorded and very accurate pressure measurements can be performed [21]. These types of experiments constitute a foundation for new design methodologies, even though they are rarely tested outside of the laboratory.

The study of explosive events in urban scenarios in a more integrative manner can be limited owing to the complex or expensive experimental and numerical tools required. The most conclusive investigative method involves conducting full-scale experiments that yield "fail/pass" results, validating a design beyond a doubt [22–24]. These experiments are usually carried out in a specifically oriented experimental field, require meticulous planning, are expensive, and usually involve long preparations [25,26]. Furthermore, the destructive nature of such experiments makes the use of accurate, delicate diagnostics problematic. To address some of these challenges, numerical simulation has found its place in the design of protective structures over recent decades. The use of a numerical simulation allows not only estimation of the developed loads on structures subjected to explosion events but also estimation of the damage caused and their dynamic responses [23,25–32]. Numerical tools are also widely used in basic and parametric studies of shock wave–structure interactions [33,34]. While powerful, numerical simulations require validation and calibration using experimental data. In complex explosive scenarios, appreciable computational power is required to resolve the loads developed on structures and structural response. Additionally, these numerical simulations cannot entirely incorporate the complicated physics involved in the shock wave reflection process and the interaction of the reflected shocks with the induced fast turbulent flow. The numerical tools used to simulate explosive events are usually based on schemes that neglect viscosity, a parameter that has been proven to be substantial in shock wave-structure interactions [25,35–40].

Another widely accepted method for studying the loads developed in explosive events is by employing small-scale experiments [41–44]. A scaled-down model is subjected to an equivalently scaled explosion, thereby simulating the full-scale scenario. This method is particularly effective since the developing loads and the structural response of the structure act on distinctively different time scales. The structural response due to the dynamic load imposed by a shock wave impingement is much slower than the load application time. Simulating the structural response, however, requires consideration of structural weight and mechanical strength effects on the small-scale response, which might prove impossible. Such attempts have been recorded previously [45]. The disadvantage of using small-scale experiments is that unique problems absent from large-scale experiments are sometimes introduced [37]. These errors are difficult to predict, and the well-known Cranz–Hopkinson "cube root" scaling law [25], which is suitable for self-similar open-field explosions, does not apply directly to urban scenarios. Nevertheless, these challenges can be overcome by careful calibration and validation. Ultimately, small-scale experiments have a strong appeal to researchers and designers because they provide a low-cost, rapid prototyping technique that, under the right circumstances, is able to provide good assessment of the loads to be expected in real large-scale scenarios [36–40,43–50].

The exploding wire (EW) technique lacks most of the safety disadvantages involved with small explosive charges commonly used in small-scale experiments. In this method, a thin metal wire is connected to a charged high-capacity electrical capacitor. The stored energy in the capacitor is then discharged through the wire, causing the wire to undergo an extremely fast heating process that causes it to melt and evaporate virtually without any volume changes. The dense, hot, vaporized metal gas expands rapidly and forms a strong blast wave [36,46,51–54].

Surveying the substantial array of studies published on the subject, one finds a lack of tools to study developing loads inside a structure given an imposed load. While there is, as mentioned, an abundance of studies concerning the propagation of shock waves inside structures and concerning the loads imposed on structures, it is difficult to find studies directly linking the two. A considerable number of works were performed on this subject on a small scale at the Ernst Mach Institute (EMI) in the 1980s–1990s, but the results were not used to link the imposed conditions and the penetrating loads [55].

In this study, the exploding wire technique was implemented to investigate how the pressure and impulse imposed at the frontal façade of a structure together with the structure's internal geometry affect the developing load on the target wall inside the structure. In the next section, a description of the studied problem is presented. A presentation of the experimental setup, results, and discussion follow, entailing the governing physical mechanisms coupled with an example in which the implications of this study prove to be beneficial for simulating large explosions in the laboratory.

2. The investigated problem

This study aims to further the understanding of the physical mechanisms determining the pressure build-up inside a structure following the impingement of an explosion-generated blast wave. Fig. 1 broadly renders the important aspects of the studied problem. The study focuses on a typical single-story building exposed to a blast wave impinging on its frontal façade. The blast wave generates initial conditions on the frontal façade of the structure, namely pressure and impulse. Typically, following the initial impingement, a weaker blast wave enters the structure through openings in the frontal façade, propagates through the structure, and reaches the back wall. Throughout its propagation, the initial wave diffracts and reflects from the internal geometry, sidewalls, and back wall. The diffracted waves reverberate inside the structure, with some pressure exhausting via the building façade openings, until the reflections eventually subside and pressure returns to its atmospheric level. The main point of interest in this study is located at the center of the target wall as seen in Fig. 1.

Resolving the three-dimensional diffraction pattern inside the complex structure is difficult and resource-consuming. Furthermore, wave propagation inside the structure and the resulting flow field depend strongly on the internal geometry. Accurately resolving the internal flow field numerically for every change of initial conditions or internal geometry would require a new solution in each case.

Rather than studying detailed flow features and reflections, this study adopts a different approach to studying the dependence of pressure build-up on important parameters. We examine the scenario presented in Fig. 1 in terms of initial conditions, internal

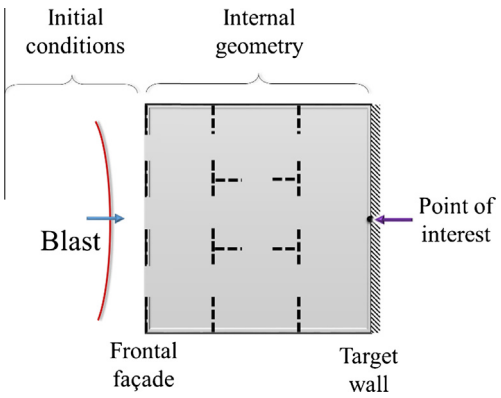

Fig. 1. A schematic description of the investigated problem.

geometry, and target wall pressure. This approach considers internal geometry (boundary conditions) as an element that modifies the initial pressure and impulse inflicted on the frontal façade and compares it to the load inflicted on the target wall.

3. Experimental setup

Fig. 2 presents the basic components of the experimental apparatus. The electrical setup depicted in Fig. 2 includes three main electrical circuits: the charging circuit and two discharge circuits. One discharge circuit includes the thin wire and a fast power switch while the other includes a power resistor for safely discharging the system if necessary. The charging circuit includes a 200-μF capacitor, a 1-MΩ charging resistor, and a 20-kV, 20-mA high-voltage power supply. The discharge process begins by opening a vacuum valve that pumps out an isolating gas from within a spark gap (SG) switch. Large currents are thereby permitted to pass across the SG switch and finally through the thin wire, causing an explosion. The total energy stored in the capacitor was limited to 10 kJ for safety reasons. More details about the system's operation and calibration can be found in [54,56].

The pressure history recording system consists of Kistler 211b3 piezoelectric transducers. The pressure transducers were connected to the data acquisition system, which consisted of a Kistler signal conditioner (model 5118B2). The data acquisition system includes a Lecroy 314A wave-jet 100 MHz 1 GS/s oscilloscope. An external trigger box captures the electromagnetic pulse generated by the discharge current and initiates the acquisition system. All experiments performed in this study used copper wires 70 mm in length and 1.1 mm in diameter. The charged capacitor voltage was 6 kV for all experiments.

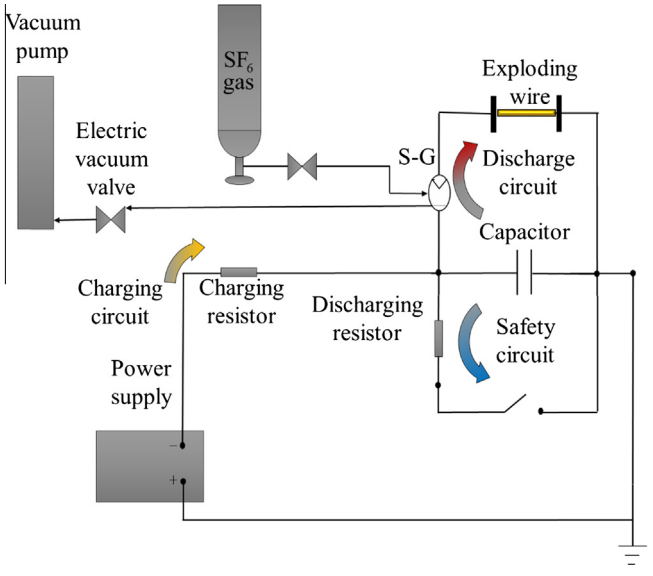

Fig. 2. A schematic description of the exploding wire system.

3.1. Repeatability

Explosions generated by the exploding wire technique are highly repeatable. The main parameters affecting explosion strength are the wire material, wire dimensions, and the energy stored in the capacitor. To check system repeatability, three experiments were conducted under the same conditions. The reflected pressure and impulse from these experiments, measured at 150 mm from the explosion, are presented in Fig. 3a and b. These results demonstrate the good repeatability of the system; hence, in the subsequent analysis each experiment appears once.

3.2. Initial conditions

Maintaining a constant explosion yield, generated from identical wires, allows for two possible ways to set the initial conditions imposed on the frontal façade of the structure (see Fig. 4). The first is by changing the frontal façade's distance from the explosion. As the distance increases, the imposed pressure and impulse decrease. Each different distance generates a change in both the pressure profile and the impulse. A second method employs a stiff reflector placed around the explosion, which channels energy toward the tested model. This method yields a different pressure–impulse combination than in the free-air case.

The reflector enabled producing initial conditions in which the peak impulse was the same as that generated by means of a free-air explosion that was initiated at a different distance. For example, one combination used in this study involved free air at 100 mm from the explosion and at 300 mm with the reflector. In these locations, peak impulses were similar, although peak over-pressures were different. Though non-intuitive, this comparative method enabled the isolation of one initial parameter: impulse or pressure.

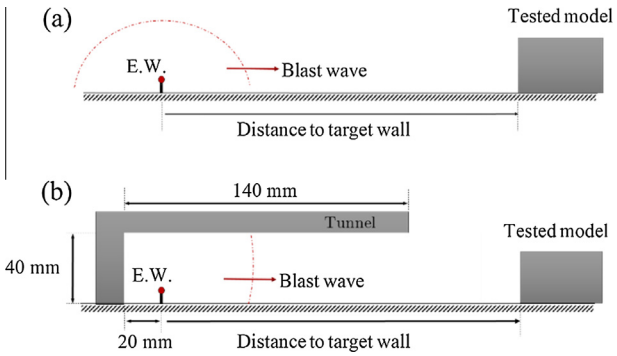

Fig. 4. Two methods were used to generate initial conditions in the present study: (a) an open-air ground-burst, and (b) a reflector placed around the explosion area.

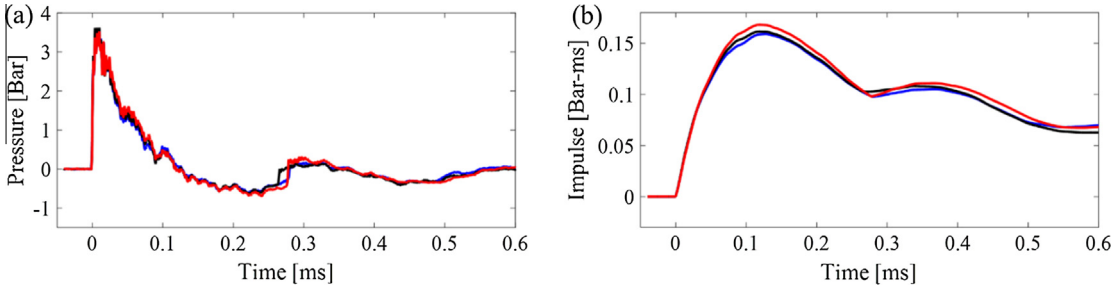

Fig. 3. Reflected pressure and impulse measured 150 mm from the explosion in three different experiments.

In a previous study, we discussed the nature of the explosions generated by the exploding wires at length [54]. Exploding wires produce initially cylindrical blast waves that decay slower than spherical ones. This study showed that in the distances discussed in the current study, the blast wave retains its cylindrical form. The wire length was 70 mm while the façade width was 92 mm in all setups. In locations where the blast strengths are similar, the cylindrical blast waves differ from the spherical by exhibiting a slower rate at which the pressure decayed following the initial impingement. However, this difference has little influence in the scope of this study, where the methodology requires loading the frontal façade of the structure by two different pressure profile in order to generate similar impulses. Furthermore, due to their cylindrical nature, using exploding wires of the same order in size as the width of the frontal façade generates uniform loading.

3.3. Internal geometry

Fig. 5 depicts four different structure configurations used in this study. Each model had the same frontal façade spanning 92 mm × 25 mm (including external walls) with three 12 mm × 10 mm equally spaced windows. The models differed as follows: Model A had no internal divisions. Model B had a 28 mm × 28 mm (internal dimensions) centered room partially obstructing the flow and located immediately behind the center window; in addition, an 8 mm × 20 mm doorway was located at the center of each internal wall. Model C had three internal rooms, each 28 mm × 28 mm (internal dimensions), placed immediately behind the frontal façade wall. A doorway connected each pair of adjoining rooms and three more doorways were placed facing the frontal façade in symmetry with the three windows. All doors were 8 mm wide and 20 mm tall. Model D was 85 mm long and had an additional row of internal rooms identical to the row of rooms in model C.

All model parts were machined from 2-mm-thick polycarbonate sheets glued together. The models were positioned with the frontal façade directly facing the exploding wire at various distances. A pressure transducer was mounted on a wall adjacent to the target wall at the door opening (see the schematic illustration in Fig. 6). The height and width of the mounting wall matched those of the structure so as not to influence the flow through formation of external reflections.

4. Results

Two sets of experiments were performed in order to study the individual influence of initial conditions and internal geometry. In the first set, the internal geometry was varied while keeping the initial conditions uniform. In the second set, each model was subjected to varying initial conditions; a model was placed at a certain location, exposed to an open-air explosion, and then moved to a farther location with the reflector so that the imposed peak impulse was similar to the one measured in the closer open-air experiments. The following sections aim to highlight the effects of each parameter.

4.1. Effects of internal geometry

Fig. 7 depicts the results obtained by exposing models A, B, and C to an open-air explosion with the model frontal façade placed at 150 mm from the explosion. Fig. 7a and b depicts the initial conditions: the pressure profile and impulse measured on the frontal façade before the effect of the internal geometry. These measurements were performed by mounting the sensor at a distance of 150 mm from the explosion without a model. Fig. 7c and d presents the measured pressure and impulse profiles at the point of interest, i.e. at the opening at the center of the target wall. To

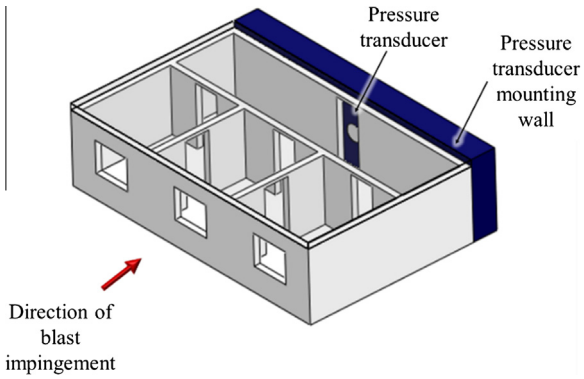

Fig. 6. A schematic description of pressure transducer positioning.

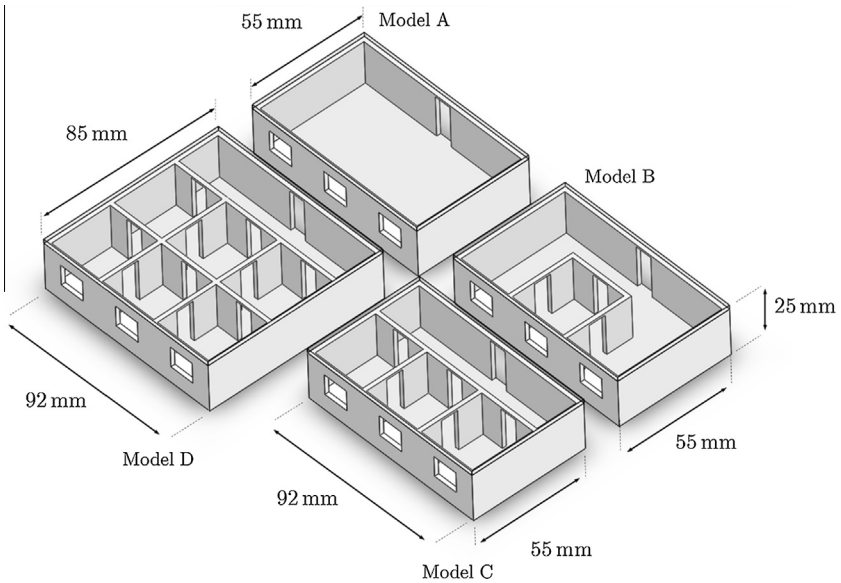

Fig. 5. Four one-story structure models ranging in size and internal geometry.

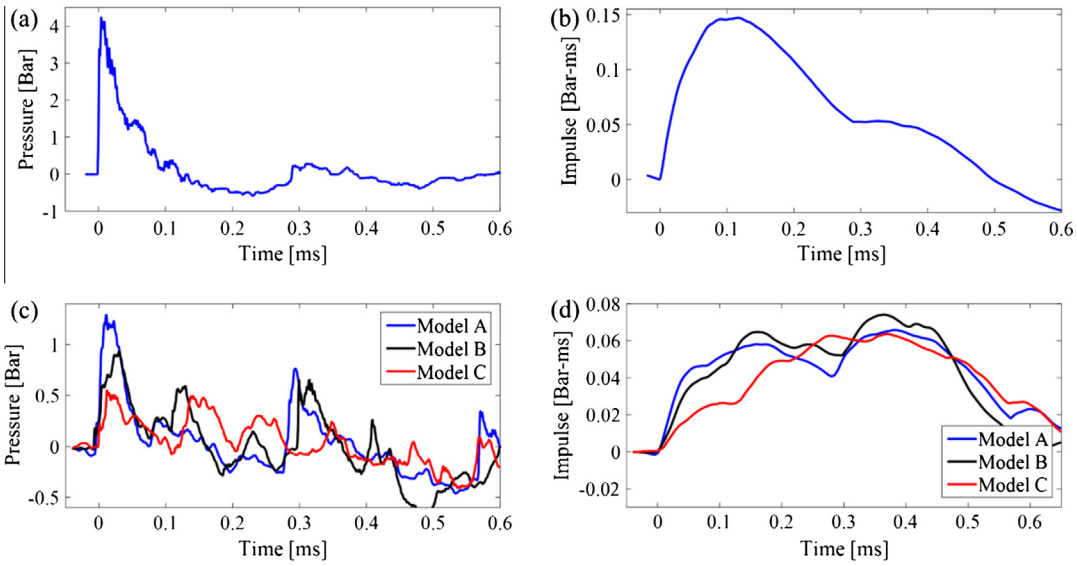

Fig. 7. Results from experiments performed with identical initial conditions and various internal geometries. (a) and (b) depict the reflected pressure and impulse developing at the frontal façade of the structures measured at 150 mm from the explosion without a model. (c) and (d) depict the pressure and impulse measured at the center of the target wall in each of the three models.

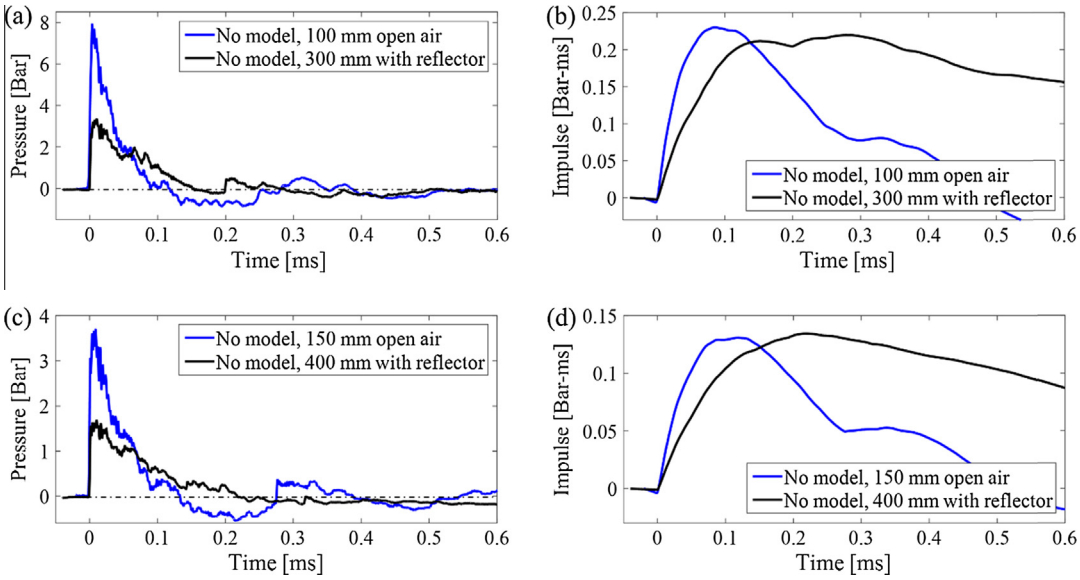

Fig. 8. Comparison of pressure–impulse combinations that were obtained in open air and with reflector explosions.

enable direct comparison between the results, all the recordings presented in this paper are shifted in time so that time $t = 0$ is when the incident wave reaches the pressure transducer.

The results in Fig. 7 show that the overall measured impulse behavior at the target wall is similar in all of the experiments. As the models become more complex, such as in Model C, there are some changes in the impulse build-up, but the overall behavior and peak impulses remain almost the same. The pressure profile at the target, on the other hand, is profoundly influenced by internal geometry. For example, Fig. 7c shows the reflection pattern through Model A, a structure without internal divisions. The initial shock was measured arriving at the target wall and then reverberates between the frontal façade and the back wall. The arrival of this trapped shock produces definitive pressure jumps where there are only weak secondary reflections from the walls reaching the measurement point in between. In experiments with Model C, a significantly more complex structure, a pressure history featuring many shock reflections was visible. These weaker pressure jumps were accompanied by many minor reflections that were probably transverse waves emanating from interactions with internal walls.

A second effect revealed in Fig. 7c is that the initial pressure jump at the target wall caused by initial shock propagation depends strongly on the complexity of the inner geometry. The peak overpressure diminishes with exceedingly complex geometries. Subsequent reflections seem to be more similar in strength between the models.

4.2. Effects of initial conditions

A second set of experiments was performed to study the effects of the initial conditions on the pressure build-up at the target wall. As stated previously, changing the distance between the exploding wire and the model frontal façade alters the initial conditions. The impulse and pressure change in different ways, and hence this method offers no comparable data. An alternative method over-

comes this limitation. A reflector, shown in Fig. 4b, focuses the blast energy, thereby providing at a certain location a peak impulse that matches that of an open-air explosion at closer range. Fig. 8 presents two combinations of open-air and focused distances. It is impossible to generate exactly the same impulse at the frontal façade, but Fig. 8 depicts two combinations that generate impulses sufficiently similar for our purposes.

The two combinations shown in Fig. 8 generated similar peak impulses on the structure while imposing very different pressure loads both in peak overpressure and duration. It is important to note that the peak impulse was reached when the positive pressure duration ended, i.e. when the pressure returned to atmospheric conditions (marked with a dashed line in Fig. 8a and c). Since the open-air explosion generated an additional negative pressure phase, the impulse declined much more rapidly. This effect, however, had little influence on conditions inside the structure since low pressure propagates inwards at a slower speed. The mass flow into the structure effectively stopped when the impulse begins to decline. Nevertheless, the moment when the negative impulse penetrated the structure and affected the experiments, i.e. the start of the impulse drop at the end-wall, effectively marks the end of the experiment since a direct comparison between the two cases is no longer valid.

The initial conditions shown in Fig. 8 were imposed on the models shown in Fig. 5 by placing the frontal façades at the same locations where they were measured (the pressure transducer mounting wall was placed at different locations accordingly). Fig. 9 depicts the overpressures and impulses measured at the target walls of Models A, B, C and D. A single set of initial conditions is presented for each model.

As expected, since the two initial impulse conditions were similar up to the peak, the impulses on the target wall are also in reasonable agreement. In the open-air experiments, the low pressure propagated into the structure and lowered the impulse after the peak as seen in the initial conditions (Fig. 8).

The pressure measurements recorded at the target walls, on the other hand, are not understood so intuitively. Despite very different initial pressures imposed on the frontal façade for the open-air and reflected conditions (up to twice the peak overpressure), the pressure profiles inside the structure were remarkably similar. In fact, the pressure profiles display similar overpressure as well as similar reflection patterns. Referring to the results shown

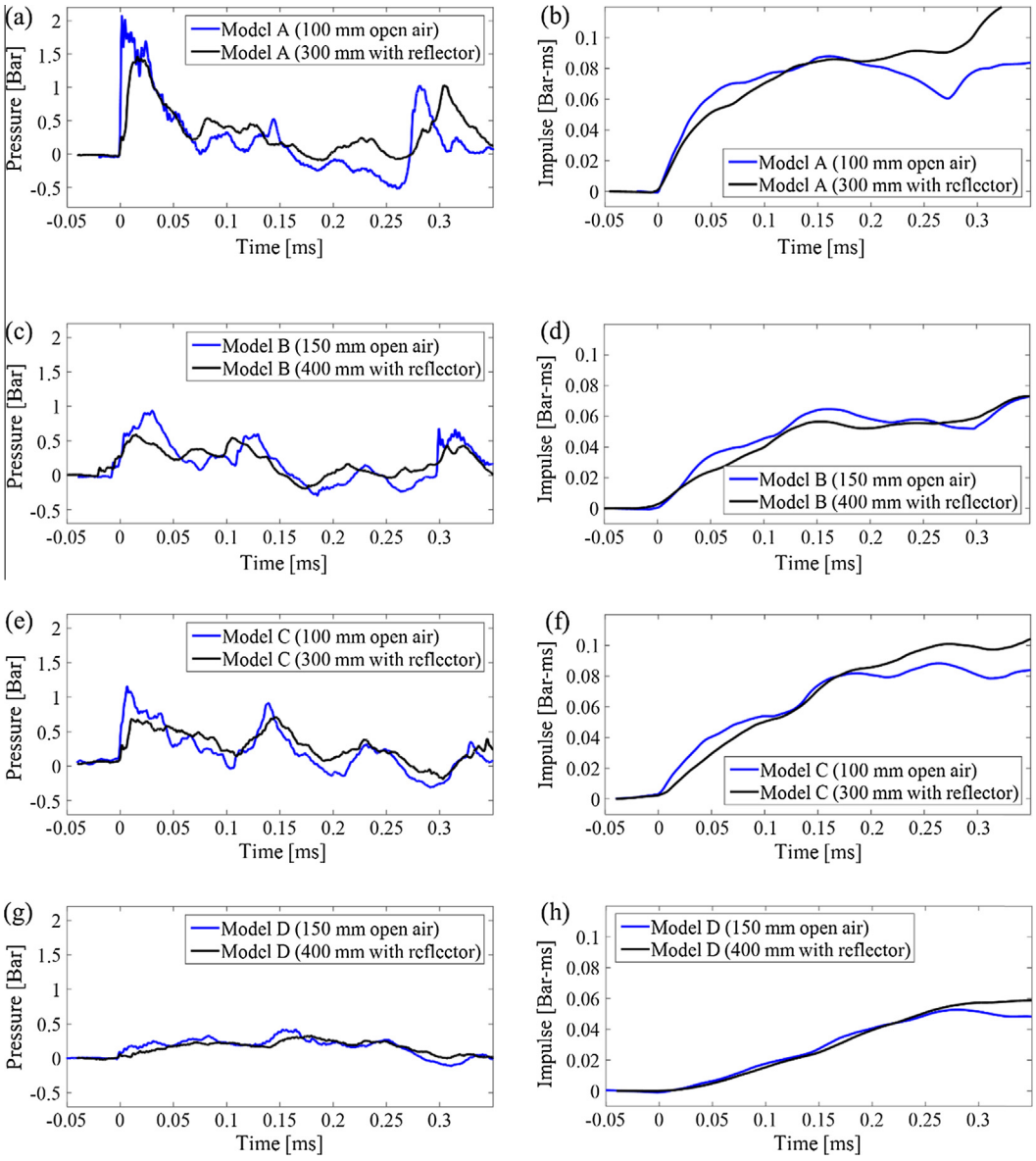

Fig. 9. Experimental results depicting the target wall pressure and impulse profiles in the various models.

in Fig. 7, imposing the same initial conditions led to matching impulses at the target wall but very different reflection patterns. In this case, the dominance of internal geometry was even more pronounced, since the reflection patterns were not only highly affected by the internal geometry but also impeded the propagation of stronger shocks inside the structure. To support this notion, a comparison between two different internal geometries shows that, as complexity increases, the pressure profiles become even more similar.

5. Discussion

5.1. The mechanism governing the pressure build-up

A better understanding of the physical mechanism governing the pressure build-up inside a structure can be achieved by making a direct comparison to recently published advances in shock wave-porous medium interaction studies. It was shown in [13,14] that, in the event of shock wave impingement on a stiff porous medium, the pressure build-up behind the porous barrier is governed by a filtration process that attenuates high-frequency pressure fluctuations. This mechanism effectively inhibits pressure build-up behind the porous barrier as the initial shock wave propagating through the porous medium interacts repeatedly with the skeleton of the porous medium. In these studies, it was argued that this governing mechanism might apply to other scenarios as long as the propagating shock is significantly diffracted.

Studying the pressure build-up profiles presented above in light of this comparison, the internal geometry can be considered a low-porosity, stiff porous medium.

To demonstrate these effects, Fig. 10 depicts a low-pass filter manipulation performed on the pressure profile inflicted in the open-air experiment on the frontal façade of Model D. The low-pass filtering was expressed by using the following first-order differential description:

$$\frac{dp_{out}}{dt} = C(P_{out}(t) - P_{in}(t)) \quad (1)$$

where P_{out} is the pressure at the target wall of the model, P_{in} is the initial pressure inflicted on the frontal façade of the model, and C is the characteristic time constant of the model. The time constant C was found by an iterative process to give the smallest impulse deviation from the experimental results.

Fig. 10 demonstrates that, while the low-pass first-order filter cannot capture sharp shock reflections, it predicts quite well the overall behavior of the recorded pressure profile. As can be expected, this prediction matches the impulse profile, as well (see Fig. 10b).

This mechanism, demonstrated here for the first time, directly explains the non-intuitive similarities found between the pressure profiles seen in Fig. 9. As the models become more complex, the amplitudes associated with strong shocks attenuate further and the effects of differences in the initial peak pressure decline dramatically. Furthermore, since the manipulation facilitated by the internal geometry is the same for both initial conditions, the output pressure profile exhibits very similar characteristics.

This analogy to stiff porous media and the higher-order effects of complex internal geometry on pressure transformation require further study. It is clear, however, that by employing this method of analysis researchers can predict the overall pressure build-up inside structures without requiring very complicated numerical simulations. It should also be stressed that, if one successfully characterizes the filtering facilitated by the internal geometry of a specific structure, the target wall pressure build-up for different initial conditions can be predicted easily.

5.2. Application to a full-scale model

The above findings have valuable implications for predicting the loads due to large-scale explosions in small-scale laboratory settings. Although very repeatable and straightforward, the EW method generates only weak explosions. A previous study showed that the system used here, i.e. exploding a 70-mm-long, 1.1-mm-diameter copper wire with a capacitor charge of 6 kV, would generate an energy equivalent to the explosion of 0.1 g of TNT [54]. Consequently, simulating large explosions in urban scenarios, such as on the scale of one ton of TNT, would necessitate scaling down to miniscule proportions. The results here provide a tool to address this problem.

To demonstrate the implications of the results shown above, a full-scale simulation of an explosion event in which an 800 kg TNT charge explodes 15 m from the frontal façade of a structure is evaluated. Fig. 11 depicts the overall dimensions of the full-scale scenario. The structure has three equally spaced 1 m × 1 m

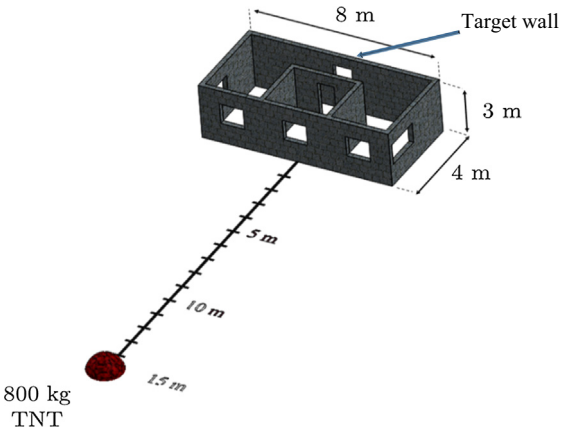

Fig. 11. The full-scale scenario in which an 800 kg hemispherical TNT charge explodes 15 m from a one-story structure's frontal façade (the roof is transparent).

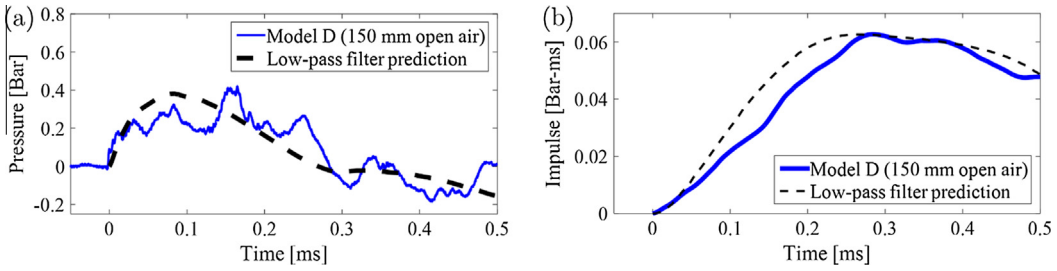

Fig. 10. A comparison between the recorded pressure (a) and impulse (b) profiles on the target wall of model D (solid lines) and the predicted pressure and impulse profiles (dashed lines) found using Eq. (1).

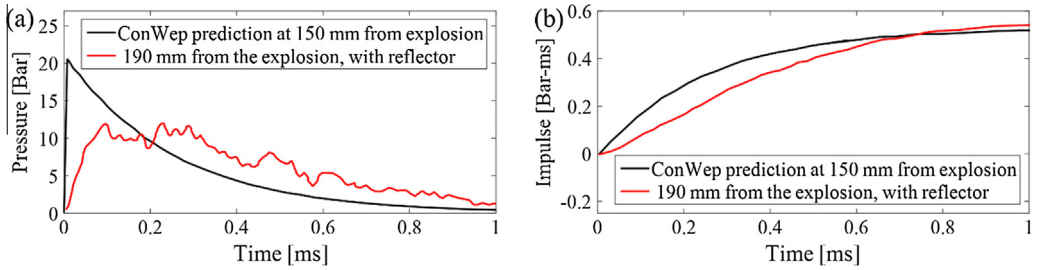

Fig. 12. Pressure and impulse profiles required to simulate an 800 kg explosion on a 1:100 scale.

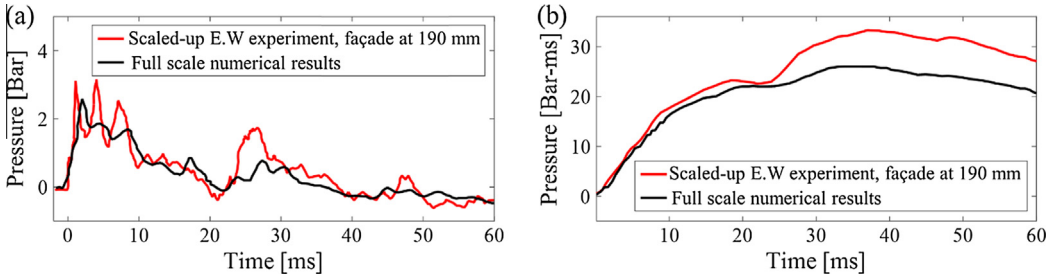

Fig. 13. A comparison between a numerical simulation and an exploding wire experiment at the target wall.

windows at its frontal façade, and two 1 m × 2 m windows at its sides. Inside, a 3 m × 3 m room was located adjacent to the frontal façade and behind the center window, partially obstructing the path to an opening in the target wall.

Fully scaling down the model (by means of the Cranz–Hopkinson law) to meet the EW system capabilities requires an impracticably small model (of a scale on the order of 1:1000). The model would be so small that the pressure transducer could not fit the opening at the target wall.

In light of this restriction, we chose a more feasible small-scale ratio of 1:100 to simulate the explosion by means of the exploding wire system. Properly simulating the explosion would further require creating a scaled-down 0.8 g hemispherical explosion at a distance of 150 mm from the frontal façade of a scaled-down model. Since we could not satisfy these conditions under the existing EW system limitations, we used the reflector and found the location where the produced impulse matched a 0.8 g TNT explosion at a 150-mm range. The desired pressures and impulses were obtained by means of the ConWep software [57]. Fig. 12 depicts the closest match that was found, which was at a distance of 190 mm from the exploding wire. As concluded in Section 4.2, we selected the distance that provided the most similar impulse.

Numerical simulations of the full-scale model were performed using MSC/Dytran commercial software. The numerical model was validated with full-scale experiments and was found to be in good agreement [58]. In order to simplify the numerical model, it was assumed that during initial wave propagation inside the structure, walls were non-deformable. The explosion was modeled as a hot air bubble burst calibrated to yield the appropriate TNT equivalent [54]. The blast loading on the building's frontal façade was validated by ConWep predictions; these also yielded satisfactory agreement.

Fig. 13 shows a comparison between the scaled-up experimental results and numerical simulations of the full-scale experiments. To display the comparison, the pressure and impulse histories from the exploding wire experiments were scaled up to the full-scale simulation according to the Cranz–Hopkinson law. In Fig. 13, the time and impulse axes are scaled by a factor of 100 while the pressure scale is unchanged.

The small-scale experiment and the numerical solution agree in both impulse and pressure behavior. It may be expected that tailoring the impulse imposed on the frontal façade should produce the proper impulse at the target wall. However, agreement between the pressure profiles was not initially expected; this can be explained based on the results presented in the previous section. The transfer of impulse through the structure along with the structure's internal geometry assured that the pressure profile was very similar to the one recorded in the simulation regardless of the incorrect pressure imposed on the frontal façade.

6. Conclusions

The current study empirically explored the effects of initial conditions and internal geometry on the pressure developing inside a typical single-story building. It was found that, when inflicting similar impulses at the frontal façade of the structure, the internal geometry determines the pressure profile that develops at the target wall regardless of the initial pressure profile.

These inferences were applied to the experimental study of a blast event in a small-scale setup. The presented findings imply that, in cases where the load developed in the interior of a complex structure due to an exterior blast event is of interest, it is satisfactory to impose the correct impulse at the frontal façade in order to acquire adequate results in terms of both impulse and pressure history inside the structure. Furthermore, as the complexity of the structure increases, the larger number of reflections facilitated by internal divisions contributes to the independence of the target wall loading from the imposed pressure profile. The results presented in this paper show the consistency of this phenomenon and will enable faster examination of protective structures in laboratory settings in the future.

The main conclusion derived in this study is that the mechanism that governs the pressure build-up on the target wall is analogous to the filtration process experienced with porous media. In previous studies [13,14], the process of filtration through a porous barrier was found to be controlled by a single parameter, namely C in Eq. (1), which as mentioned earlier is a characteristic time

constant. Extending this concept to the results found in the present study, it was shown that the effects of the structure can be characterized by a single time constant that encapsulates the structure's first-order effects and effectively determines the pressure build-up process within. The outcome of this constant's scaling properties can be exploited to rapidly predict the pressure and impulse developed on a target wall within a full-scale structure. The procedure for estimating the time constant of the full-scale structure enables the use of a small-scale experiment employing any available load profile.

Recalling that, according to the Cranz–Hopkinson scaling law, the scaling factor used in this study was 1/100, the scale of the model was calculated according to:

$$X_{small\,scale} = SF \cdot X_{full\,scale} \tag{2}$$

where X denotes any dimension and SF is the scaling factor.

The time constant can be obtained using the procedure described in Section 5.1 and a scaling factor can be used to calculate the time constant in the full-scale system according to:

$$C_{full\,scale} = \frac{C_{small\,scale}}{SF} \tag{3}$$

After determining the time constant for the full-scale system, it is possible to estimate the developed pressure and impulse on the target wall induced by any load impinging on the structure (using different charges at different distances). The load can be estimated from field experiments or via software such as ConWep [57]. This result, shown here for the first time, requires further validation.

Acknowledgments

This study was partially supported by the Israel Ministry of Defense through grant number 4440507635 635.

O. Ram is supported by the Adams Scholarship program of the Israeli Academy of Science. The authors thank Prof. G. Ben-Dor and Dr. Eytan Kochavi for their constructive discussions.

References

[1] F. Ohtomo, K. Ohtani, K. Takayama, Attenuation of shock waves propagating over arrayed baffle plates, Shock Waves 14 (2005) 379–390, http://dx.doi.org/10.1007/s00193-005-0282-5.
[2] S. Berger, O. Sadot, G. Ben-Dor, Experimental investigation on the shock-wave load attenuation by geometrical means, Shock Waves 20 (2009) 29–40, http://dx.doi.org/10.1007/s00193-009-0237-3.
[3] S. Berger, G. Ben-Dor, O. Sadot, Numerical investigation of shock wave attenuation by geometrical means: double barrier configuration, J. Fluids Eng. 137 (2014) 041203, http://dx.doi.org/10.1115/1.4028875.
[4] S. Berger, G. Ben-Dor, O. Sadot, Experimental and numerical investigations of shock-wave attenuation by geometrical means: a single barrier configuration, Eur. J. Mech. – B/Fluids 50 (2015) 60–70, http://dx.doi.org/10.1016/j.euromechflu.2014.11.006.
[5] B. Skews, Shock wave interaction with porous plates, Exp. Fluids 39 (2005) 875–884, http://dx.doi.org/10.1007/s00348-005-0023-7.
[6] A. Britan, O. Igra, G. Ben-Dor, H. Shapiro, Shock wave attenuation by grids and orifice plates, Shock Waves 16 (2006) 1–15, http://dx.doi.org/10.1007/s00193-006-0019-0.
[7] A. Britan, A.V. Karpov, E.I. Vasilev, O. Igra, G. Ben-Dor, E. Shapiro, Experimental and numerical study of shock wave interaction with perforated plates, J. Fluids Eng. 126 (2004) 399, http://dx.doi.org/10.1115/1.1758264.
[8] S. Seeraj, B.W. Skews, Dual-element directional shock wave attenuators, Exp. Therm. Fluid Sci. 33 (2009) 503–516, http://dx.doi.org/10.1016/j.expthermflusci.2008.11.002.
[9] G.S. Langdon, G.N. Nurick, N.J. du Plessis, The influence of separation distance on the performance of perforated plates as a blast wave shielding technique, Eng. Struct. 33 (2011) 3537–3545, http://dx.doi.org/10.1016/j.engstruct.2011.07.017.
[10] A. Levy, G. Ben-Dor, B.W. Skews, S. Sorek, Head-on collision of normal shock waves with rigid porous materials, Exp. Fluids 15 (1993), http://dx.doi.org/10.1007/BF00189885.
[11] A. Levy, D. Levi-Hevroni, S. Sorek, G. Ben-Dor, Derivation of Forchheimer terms and their verification by application to waves propagation in porous media, Int. J. Multiph. Flow 25 (1999) 683–704, http://dx.doi.org/10.1016/S0301-9322(98)00031-7.
[12] A. Levy, G. Ben-Dor, S. Sorek, Numerical investigation of the propagation of shock waves in rigid porous materials: development of the computer code and comparison with experimental results, J. Fluid Mech. 324 (2006) 163, http://dx.doi.org/10.1017/S0022112096007872.
[13] O. Ram, O. Sadot, A simple constitutive model for predicting the pressure histories developed behind rigid porous media impinged by shock waves, J. Fluid Mech. 718 (2013) 507–523, http://dx.doi.org/10.1017/jfm.2012.627.
[14] O. Ram, O. Sadot, Analysis of the pressure buildup behind rigid porous media impinged by shock waves in time and frequency domains, J. Fluid Mech. 779 (2015) 842–858, http://dx.doi.org/10.1017/jfm.2015.463.
[15] E. Del Prete, A. Chinnayya, L. Domergue, A. Hadjadj, J.-F. Haas, Blast wave mitigation by dry aqueous foams, Shock Waves 23 (2012) 39–53, http://dx.doi.org/10.1007/s00193-012-0400-0.
[16] A. Britan, G. Ben-Dor, H. Shapiro, M. Liverts, I. Shreiber, Drainage effects on shock wave propagating through aqueous foams, Colloids Surf. A: Physicochem. Eng. Aspects 309 (2007) 137–150, http://dx.doi.org/10.1016/j.colsurfa.2007.01.018.
[17] A. Britan, M. Liverts, G. Ben-Dor, Shock wave propagation through wet particulate foam, Colloids Surf. A: Physicochem. Eng. Aspects 382 (2011) 145–153, http://dx.doi.org/10.1016/j.colsurfa.2011.01.019.
[18] A. Britan, G. Ben-Dor, T. Elperin, O. Igra, J.P. Jiang, Gas filtration during the impact of weak shock waves on granular layers, Int. J. Multiph. Flow 23 (1997) 473–491, http://dx.doi.org/10.1016/S0301-9322(96)00088-2.
[19] A. Britan, G. Ben-Dor, O. Igra, H. Shapiro, Shock waves attenuation by granular filters, Int. J. Multiph. Flow 27 (2001) 617–634, http://dx.doi.org/10.1016/S0301-9322(00)00048-3.
[20] A. Britan, H. Shapiro, G. Ben-Dor, The contribution of shock tubes to simplified analysis of gas filtration through granular media, J. Fluid Mech. 586 (2007) 147, http://dx.doi.org/10.1017/S0022112007006878.
[21] O. Igra, J. Falcovitz, L. Houas, G. Jourdan, Review of methods to attenuate shock/blast waves, Prog. Aerosp. Sci. 58 (2013) 1–35, http://dx.doi.org/10.1016/j.paerosci.2012.08.003.
[22] A. Schenker, I. Anteby, E. Gal, Y. Kivity, E. Nizri, O. Sadot, et al., Full-scale field tests of concrete slabs subjected to blast loads, Int. J. Impact Eng. 35 (2008) 184–198, http://dx.doi.org/10.1016/j.ijimpeng.2006.12.008.
[23] W. Riedel, K. Fischer, C. Kranzer, J. Erskine, R. Cleave, D. Hadden, et al., Modeling and validation of a wall-window retrofit system under blast loading, Eng. Struct. 37 (2012) 235–245, http://dx.doi.org/10.1016/j.engstruct.2011.12.015.
[24] D. Yankelevsky, S. Schwarz, B. Brosh, Full scale field blast tests on reinforced concrete residential buildings – from theory to practice, Int. J. Prot. Struct. 4 (2013) 565–590, http://dx.doi.org/10.1260/2041-4196.4.4.565.
[25] C.E. Needham, Blast Waves, Springer Science & Business Media, 2010.
[26] P.W. Weber, K.K. Millage, J.E. Crepeau, H.J. Happ, Y. Gitterman, C.E. Needham, Numerical simulation of a 100-ton ANFO detonation, Shock Waves 25 (2014) 127–140, http://dx.doi.org/10.1007/s00193-014-0547-y.
[27] B. Luccioni, D. Ambrosini, R. Danesi, Blast load assessment using hydrocodes, Eng. Struct. 28 (2006) 1736–1744, http://dx.doi.org/10.1016/j.engstruct.2006.02.016.
[28] J.K. Clutter, J.T. Mathis, M.W. Stahl, Modeling environmental effects in the simulation of explosion events, Int. J. Impact Eng. 34 (2007) 973–989, http://dx.doi.org/10.1016/j.ijimpeng.2006.03.003.
[29] N. Gebbeken, T. Döge, Explosion protection—architectural design, urban planning and landscape planning, Int. J. Prot. Struct. 1 (2010) 1–22, http://dx.doi.org/10.1260/2041-4196.1.1.1.
[30] C. Wu, M. Lukaszewicz, K. Schebella, L. Antanovskii, Experimental and numerical investigation of confined explosion in a blast chamber, J. Loss Prev. Process Ind. 26 (2013) 737–750, http://dx.doi.org/10.1016/j.jlp.2013.02.001.
[31] C. Amadio, C. Bedon, Viscoelastic spider connectors for the mitigation of cable-supported façades subjected to air blast loading, Eng. Struct. 42 (2012) 190–200, http://dx.doi.org/10.1016/j.engstruct.2012.04.023.
[32] D. Ambrosini, B. Luccioni, A. Jacinto, R. Danesi, Location and mass of explosive from structural damage, Eng. Struct. 27 (2005) 167–176, http://dx.doi.org/10.1016/j.engstruct.2004.09.003.
[33] S.L. Krahe, M.A. Franks, P.D. Smith, T.A. Rose, Façade failure effects on blast propagation along city streets, Proc. ICE – Struct. Build. 156 (2003) 359–365, http://dx.doi.org/10.1680/stbu.2003.156.4.359.
[34] A.M. Benselama, M.J.-P. William-Louis, F. Monnoyer, C. Proust, A numerical study of the evolution of the blast wave shape in tunnels, J. Hazard. Mater. 181 (2010) 609–616, http://dx.doi.org/10.1016/j.jhazmat.2010.05.056.
[35] T. Rose, P. Smith, Influence of the principal geometrical parameters of straight city streets on positive and negative phase blast wave impulses, Int. J. Impact Eng. 27 (2002) 359–376, http://dx.doi.org/10.1016/S0734-743X(01)00060-4.
[36] A. Zyskowski, I. Sochet, G. Mavrot, P. Bailly, J. Renard, Study of the explosion process in a small scale experiment—structural loading, J. Loss Prev. Process Ind. 17 (2004) 291–299, http://dx.doi.org/10.1016/j.jlp.2004.05.003.
[37] S. Rahman, E. Timofeev, H. Kleine, Pressure measurements in laboratory-scale blast wave flow fields, Rev. Sci. Instrum. 78 (2007) 125106, http://dx.doi.org/10.1063/1.2818807.
[38] K. Cheval, O. Loiseau, V. Vala, Laboratory scale tests for the assessment of solid explosive blast effects. Part I: Free-field test campaign, J. Loss Prev. Process Ind. 23 (2010) 613–621, http://dx.doi.org/10.1016/j.jlp.2010.05.001.
[39] K. Cheval, O. Loiseau, V. Vala, Laboratory scale tests for the assessment of solid explosive blast effects. Part II: Reflected blast series of tests, J. Loss Prev. Process Ind. 25 (2012) 436–442, http://dx.doi.org/10.1016/j.jlp.2011.11.008.
[40] I. Sochet, P.E. Sauvan, R. Boulanger, F. Nozeres, Effect of a gas charge explosion at the closed end of a gas storage system, J. Loss Prev. Process Ind. 27 (2014) 42–48, http://dx.doi.org/10.1016/j.jlp.2013.10.003.

[41] K. Ohashi, H. Kleine, K. Takayama, Characteristics of blast waves generated by milligram charges, in: Am. Phys. Soc. 53rd Annu. Meet. Div. Fluid Dyn., Washington, DC, 2000.
[42] G.S. Settles, Fluid mechanics and homeland security, Annu. Rev. Fluid Mech. 38 (2006) 87–110, http://dx.doi.org/10.1146/annurev.fluid.38.050304.092111.
[43] H. Reichenbach, In the footsteps of Ernst Mach – a historical review of shock wave research at the Ernst-Mach-Institut, Shock Waves 2 (1992) 65–79, http://dx.doi.org/10.1007/BF01415894.
[44] P.D. Smith, G.C. Mays, T.A. Rose, K.G. Teo, B.J. Roberts, Small scale models of complex geometry for blast overpressure assessment, Int. J. Impact Eng. 12 (1992) 345–360, http://dx.doi.org/10.1016/0734-743X(92)90112-7.
[45] A. Brill, Y. Me-Bar, M. Siman, O. Sadot, G. Ben-Dor, Diaphragm gauge for measuring explosive impulse, Int. J. Impact Eng. 38 (2011) 765–769, http://dx.doi.org/10.1016/j.ijimpeng.2011.04.003.
[46] R.R. Buntzen, The use of exploding wires in the study of small-scale underwater explosions, in: W. Chace, H. Moore (Eds.), Exploding wires proceedings, vol. 2, Plenum press, New York, 1995, pp. 195–205, http://dx.doi.org/10.1007/978-1-4684-7505-0_16.
[47] K. Spranghers, I. Vasilakos, D. Lecompte, H. Sol, J. Vantomme, Numerical simulation and experimental validation of the dynamic response of aluminum plates under free air explosions, Int. J. Impact Eng. 54 (2013) 83–95, http://dx.doi.org/10.1016/j.ijimpeng.2012.10.014.
[48] F.D. Bennett, Cylindrical shock waves from exploding wires, Phys. Fluids 1 (1958) 347, http://dx.doi.org/10.1063/1.1705893.
[49] W.L. Fourney, U. Leiste, R. Bonenberger, D.J. Goodings, Mechanism of loading on plates due to explosive detonation, Fragblast 9 (2005) 205–217, http://dx.doi.org/10.1080/13855140500431989.
[50] P.D. Smith, P. Vismeg, L.C. Teo, L. Tingey, Blast wave transmission along rough-walled tunnels, Int. J. Impact Eng. 21 (1998) 419–432, http://dx.doi.org/10.1016/S0734-743X(98)00003-7.
[51] F.D. Bennett, Shock-producing mechanisms for exploding wires, Phys. Fluids 5 (1962) 891, http://dx.doi.org/10.1063/1.1706704.
[52] F.D. Bennett, Energy partition in the exploding wire phenomena, Phys. Fluids 1 (1958) 515, http://dx.doi.org/10.1063/1.1724375.
[53] A. Grinenko, S. Efimov, A. Fedotov, Y.E. Krasik, I. Schnitzer, Efficiency of the shock wave generation caused by underwater electrical wire explosion, J. Appl. Phys. 100 (2006) 113509, http://dx.doi.org/10.1063/1.2395603.
[54] O. Ram, O. Sadot, Implementation of the exploding wire technique to study blast-wave–structure interaction, Exp. Fluids 53 (2012) 1335–1345, http://dx.doi.org/10.1007/s00348-012-1339-8.
[55] H. Reichenbach, P. Neuwald, Fluid-dynamics of Explosions in Multi-chamber Systems Phenomenology Test Program, Ernst-Mach Institute, Freiburg Im Breisgau, Germany, 2000.
[56] O. Ram, B. Ostraich, O. Sadot, A novel experimental system for blast structure interaction research, in: K. Kontis (Ed.), 28th Int. Symp. Shock Waves SE – 16, Springer, Berlin Heidelberg, 2012, pp. 105–110, http://dx.doi.org/10.1007/978-3-642-25688-2_16.
[57] U. S. Army Engineer Waterways Experiment Station, ConWep, 1992, Conventional Weapons Effects n.d.
[58] B. Ostraich, Y. Kivity, I. Anteby, O. Sadot, G. Ben-Dor, Load assessment on safe rooms doors report, Shock Tube Laboratory, Protective Technologies R&D Center, Faculty of Engineering Sciences, Ben-Gurion University of the Negev, Beer-Sheva, Israel, 2009.